https://doi.org/10.53360/2788-7995-2025-2(18)-62

IRSTI: 81.33.29

R. Kenzhegalieva, M.Zholdybayev, N.Akatyev*
M. Utemisov West Kazakhstan University,
090000, Republic of Kazakhstan, Uralsk, N. Nazarbayev Ave. 162
*e-mail: nikolay.akatyev@wku.edu.kz

SYNERGISTIC EFFECT OF 1,2-PHENYLENEDIAMINE AND DISODIUM NAPHTHALENE-1,5-SULFONATE FOR ENHANCED CORROSION PROTECTION OF CARBON STEEL IN 0.5 M H_2SO_4 SOLUTION: EXPERIMENTAL AND THEORETICAL INSIGHTS

Annotation: *This work investigates the corrosion inhibition of carbon steel in 0.5 mol·dm* $^{-3}$ H_2SO_4 *using a binary system of 1,2-phenylenediamine and disodium naphthalene-1,5-sulfonate. Experimental techniques, including weight loss assay, electrochemical methods, and surface analysis, demonstrated significant inhibition efficiency, reaching 88.43% under optimal conditions. The synergistic effect between the two components was evaluated as 2.59, indicating enhanced performance compared to individual components. Computational studies using molecular dynamics and DFT revealed strong interactions, driven by the formation of hydrogen bonding promoted by electrostatic forces during adsorption, which stabilize the protective layer on the metal surface. The adsorption mechanism was consistent with the Langmuir adsorption model, and obtained thermodynamic parameters confirmed spontaneous physisorption of the inhibitor. Electrochemical results identified the binary system as a mixed-type inhibitor, effectively reducing both anodic and cathodic corrosion processes. These findings provide valuable insights into the design of synergistic inhibitor systems for industrial applications.*

Key words: *metal protection, synergistic effect, corrosion inhibitors, inhibition efficiency, molecular dynamics, reactivity descriptors.*

INTRODUCTION

In modern corrosion science, the development of corrosion inhibitors is guided by several key principles. The most common strategy is combining multiple inhibitors to achieve synergistic effects. This approach enhances the overall inhibition efficiency by targeting both anodic and cathodic reactions [1]. The synergetic strategy for developing new corrosion inhibitors involves combining two or more substances to achieve enhanced corrosion protection through cooperative interactions. This approach leverages the complementary properties of different components, leading to higher inhibition efficiency than individual inhibitors alone. Such systems are very diverse and may contain organic and inorganic components, both of synthetic and natural origin [2]. Synergistic mixtures often reduce the required concentration of each component, lowering costs while maintaining high inhibition efficiency [3]. Synergistic systems can be tailored for specific environments, such as acidic, saline, or high-temperature conditions, making them versatile for industries like oil and gas, marine, and construction [4]. Techniques like molecular dynamics simulations and density functional theory (DFT) enable the prediction and optimization of synergistic interactions, accelerating the development process [5].

Synergistic inhibitors are widely used to protect pipelines, storage tanks, and drilling equipment. For instance, combinations of organic inhibitors (e.g., imidazolines) with inorganic salts (e.g., zinc or phosphate ions) are employed to prevent corrosion in acidic and saline conditions. Recent research has shown that the cation-rich and anion-rich catanionic mixtures of cetyltrimethylammonium bromide (CTAB) and sodium dodecyl sulfate (SDS), as corrosion inhibitor of mild steel, in aqueous solution of 3.5% NaCl. Mixed inhibitor demonstrates more appropriate inhibition properties compared to the solutions of the individual surfactants, due to strong adsorption on the metal surface and formation of a protective film [6]. The synergistic inhibition effect of sodium phytate and benzotriazole on 20SiMn steel in 3.5% NaCl solutions was studied by Cao using experimental and theoretical approaches. Results indicate that a protective double-layered film is formed with the presence of the mixture of these compounds. The inhibition efficiency of the mixed inhibitor was found to be 99.12%, with a synergism parameter of 3.62 [7].

In this case, our study focuses on synthesizing and evaluating the anticorrosive properties of binary systems based on aromatic amines and sulfonic acid salts. Aromatic amines enhance adsorption through nitrogen-containing functional groups, while sulfonates improve solubility and electrochemical stability [8]. These systems form *in situ* via electrostatic interactions between protonated amines and sulfonate anions, leading to the formation of ionic pairs that enhance adsorption and create a more stable protective layer. The inhibition efficiency and structural properties of these systems were investigated using theoretical (PM3 and DFT) and experimental (gravimetric and electrochemical) methods, comparing individual components and their binary compositions in a 1:1 molar ratio.

EXPERIMENTAL DETAILS

Reagent and materials

All analytical-grade reagents were bought from commercial suppliers and used without any further purification. The ST3SP2-GP2 (GOST 535-2005) carbon steel specimens used for the corrosion tests with the following chemical compositions (ω%): C – 0.22, Mn – 0.65, Si – 0.3, P – 0.04, S – 0.05, Cr – 0.3, Ni – 0.3, Cu – 0.3, N – 0.01, As – 0.08, and the remainder – Fe.

Weight loss (gravimetric) measurements

The preparation of metal coupons and the weight loss experiment were carried out as we previously reported [9]. Corrosion rate (CR, $g \cdot m^{2} \cdot h^{-1}$) was calculated as follows:

$$CR = \frac{m_1 - m_2}{S \cdot \tau} \qquad (1)$$

where m_1 and m_2 are the masses of the steel specimens before and after immersion respectively, g; S – metal specimen surface area, m^2; τ – exposure time, h.

The inhibition efficiency (IE%) was calculated using the following equation:

$$IE(\%) = \frac{CR_0 - CR_{inh}}{CR_0} \cdot 100 \qquad (2)$$

where CR_0 and CR_{inh} are the corrosion rates in the absence and in the presence of an inhibitor in $g \cdot m^{-2} \cdot h^{-1}$, respectively.

The degree of surface coverage (θ) was calculated as the following ratio:

$$\theta = \frac{IE}{100} \qquad (3)$$

Activation parameters and effect of temperature.

Activation energy values were calculated in accordance with the Arrhenius equation as follows:

$$\log\frac{CR_2}{CR_1} = \frac{E_a}{2.303R} \cdot \left(\frac{1}{T_1} - \frac{1}{T_2}\right) \qquad (4)$$

where CR_1 and CR_2 – corrosion rates of carbon steel ($g \cdot m^{-2} \cdot h^{-1}$) at T_1 and T_2 respectively, E_a – activation energy, R – universal gas constant (8.314 $J \cdot mol^{-1} \cdot K^{-1}$), T- absolute temperature.

The heat of adsorption (Q_{ads}) of the inhibitor on the metal surface was evaluated for the trend of surface coverage with temperature using the following equation (5):

$$Q_{ads} = 2.303R\left(\log\frac{\theta_2}{1-\theta_2} - \log\frac{\theta_1}{1-\theta_1}\right) \cdot \left(\frac{T_1 \cdot T_2}{T_2 - T_1}\right) \qquad (5)$$

Adsorption and thermodynamics.

In our study, the Langmuir adsorption model was used to describe the mechanism of adsorption of the developed inhibitor in accordance with the following mathematical representation:

$$\frac{C_{inh}}{\theta} = \frac{1}{K_{ads}} + C_{inh} \qquad (6)$$

where C_{inh}, $g \cdot dm^{-3}$ – inhibitor concentration, θ – degree of surface coverage, K_{ads} – the equilibrium constant for adsorption-desorption processes.

The relationship between the Gibbs free energy and the equilibrium constant of the adsorption process was determined by the equation:

$$\Delta G^0_{ads} = -RTln(55.5K_{ads}) \qquad (7)$$

where ΔG^0_{ads} is the Gibbs free energy, $kJ \cdot mol^{-1}$; R – universal gas constant (8.314 $J \cdot K^{-1} \cdot mol^{-1}$); T – absolute temperature, K; 55.5 – molar concentration of water, $mol \cdot l^{-1}$.

Electrochemical experiment

Electrochemical test was carried out using Autolab PGSTAT 101 Metrohm potentiostat/galvanostat with three electrode cells as we previously reported [10]. The calculation of inhibition efficiency through polarization resistance (IE_R/%) was derived using the equation (8):

$$IE_R = \frac{R_p^{inh} - R_p^0}{R_p^{inh}} \cdot 100 \qquad (8)$$

where R_p^{inh} and R_p^0 represent the charge transfer resistance with and without inhibitor respectively, Ω.

Computational details

The interaction of organic ions in solution, such as sulfonates and protonated amines, was also studied using computational techniques. All quantum chemical calculations were performed on a desktop PC with Windows 11, a 12th generation Intel (R) Core (TM) i7-12700H (2.30 GHz, 16 GB RAM) with GAMESS software [11]. Initially, full geometry optimization was achieved using the Molecular Mechanics (MM+) force field. The results from MM+ were used for final optimization using the semi-empirical PM3 method to obtain the equilibrium geometry and total energy (E_{tot}) of model systems. The PM3 method was used because the alternative method, AM1, has limitations in accurately modelling hydrogen bonding, electrostatic interactions, and systems with charged species, which are critical for studying ion pair interactions. The interaction energy (E_{int}) for two-component systems was calculated as follows:

$$E_{int} = E_{tot} - (E_{protonated\ amine} + E_{sulphonate\text{-}ion}) \qquad (9)$$

The quantum chemical study of the most efficient system was carried out using DFT/B3LYP/6-311+G(d,p) method. The calculations were performed as described above, and then a more accurate optimization and calculations using the chosen DFT method was used. All calculations were done for the aqueous phase because the electrochemical corrosion always appears in an aqueous medium. The solvent (H_2O) was incorporated *via* the Conductor-like Screening Model (COSMO) [12].

Molecular dynamics (MD) simulation

Molecular dynamics is used to study the mechanisms of adsorption, the energy of interactions, and the stability of the protective layer of the inhibitor. The MD simulations were carried out by using the GROMACS 2020.4 software [13]. Adsorption energy was calculated by Equation (10):

$$E_{\text{adsorption}} = E_{\text{total}} - (E_{\text{Fe(110)}} + E_{\text{inhibitor}}) \qquad (10)$$

where $E_{\text{adsorption}}$ is the adsorption energy (or interaction energy), E_{total} is the total energy of the whole system, $E_{\text{Fe(110)}}$ is the energy of the metal and $E_{\text{inhibitor}}$ is the energy of the inhibitor molecule.

The binding energy is regarded as the reciprocal of the adsorption energy of the inhibitor molecule as follows (11):

$$E_{\text{binding}} = -E_{\text{adsorption}} \qquad (11)$$

where E_{binding} is the binding energy.

The Fe (110) metal structure was chosen due to its lowest surface energy, thermodynamic stability and the largest area of the Fe crystal [14].

Synergistic effect

Synergistic effect (S) for two-component systems was calculated as follows:

$$S = \frac{IE_A + IE_B}{IE_{A+B}} \qquad (12)$$

where IE_A and IE_B – inhibition efficiencies (%) of individual components A and B respectively, and IE_{A+B} denotes inhibition efficiency of mixture A and B.

RESULTS AND DISCUSSION

Determination of the most effective inhibitory system

A theoretical and experimental approaches were used to determine the most effective anticorrosive system. Protonated amines, naphthalene sulfonates (NS) and their binary systems were studied at a molar ratio of 1:1. The total concentration of the inhibitor remained constant ($1 \cdot 10^{-3}$ mol·dm^{-3}). The weight loss assay was used to evaluate the corrosion rate (CR), the inhibition efficiency (IE), and the degree of surface coverage (θ). The total energy (E_{tot}) of each system was calculated for a theoretical evaluation using the semiempirical PM3 method. The interaction energies (E_{int}) were calculated for two-component systems using Eq.9. Synergistic effect (S) for two-component systems was obtained with Eq.10.The results obtained by both methods and calculated values of synergistic effect (S) for two-component systems are summarized in Table 1.

Table 1 – Corrosion rate (CR), inhibition efficiency (IE), degree of surface coverage (θ) and synergistic effect (S) obtained from gravimetric experiment for 24 hours of immersion in 0.5 mol·dm^{-3} H_2SO_4, and total energy (E_{tot}) and interaction energy (E_{int}) of the model systems calculated with semi-empirical (PM3) level of theory.

№	**Protonated amine**	**NS**	**E_{tot}, kcal·mol^{-1}**	**E_{int}, kcal·mol^{-1}**	**CR, g·m^{-2}·h^{-1}**	**IE%**	**θ**	**S**
1	**-**	**-**	-	-	15,87	-	-	-
2	Aniline	-	175,07	-	6,88	56,64	0,5664	-
3	1.2-PDA*	-	425,34	-	10,28	35,23	0,3523	-
4	1.3-PDA	-	404,62	-	10,93	31,28	0,3128	-
5	1.4-PDA	-	402,11	-	11,67	26,43	0,2643	-
6	Benzidine	-	393,84	-	9,16	42,26	0,4226	-
7	-	α-	-113,62	-	9,26	41,26	0,4126	-
8	-	β-	-117,14	-	7,28	54,15	0,5415	-
9	-	1,5-	-225,26	-	10,61	33,15	0,3315	-
10	-	2,6-	-238,50	-	7,11	55,18	0,5518	-
11	Aniline	α-	-33,70	-95,15	8,23	48,51	0,4851	0,49
12	Aniline	β-	-38,95	-96,88	6,86	56,75	0,5675	0,51
13	Aniline	1,5-	-183,76	-133,56	6,34	60,04	0,6004	0,67
14	Aniline	2,6-	-191,25	-127,83	7,18	54,78	0,5478	0,49
15	1.2-PDA	α-	106,56	-205,15	7,39	53,46	0,5346	0,69
16	1.2-PDA	β-	95,79	-212,41	8,21	48,25	0,4825	0,54
17	1.2-PDA	1,5-	-92,24	-292,32	2,85	82,01	0,8201	2.59
18	1.2-PDA	2,6-	-90,55	-277,38	10,49	33,88	0,3388	0,37
19	1.3-PDA	α-	110,85	-180,15	8,35	47,34	0,4734	0,65
20	1.3-PDA	β-	107,26	-180,22	8,03	49,37	0,4937	0,58
21	1.3-PDA	1,5-	-87,62	-266,97	5,20	67,38	0,6738	1,05
22	1.3-PDA	2,6-	-90,55	-256,68	8,21	48,65	0,4865	0,56
23	1.4-PDA	α-	128,47	-160,01	9,20	42,08	0,4208	0,62
24	1.4-PDA	β-	124,91	-160,06	8,13	48,78	0,4878	0,61
25	1.4-PDA	1,5-	-50,56	-227,40	8,16	48,55	0,4855	0,81
26	1.4-PDA	2,6-	-51,98	-215,59	6,39	59,73	0,5973	0,73
27	Benzidine	α-	139,05	-141,16	6,00	62,34	0,6234	0,75
28	Benzidine	β-	140,22	-136,48	6,44	59,42	0,5942	0,62
29	Benzidine	1,5-	-33,96	-202,54	6,66	58,06	0,5806	0,77
30	Benzidine	2,6-	-35,82	-191,16	8,86	44,18	0,4418	0,45

** – phenylenediamine (PDA)*

Table 1 shows that the system consisting of diprotonated 1,2-phenylenediamine (1.2-PDAH_2^{2+}) and naphthalene-1,5-disulfonate (1.5-NDS^{2-}) (1 : 1) has the lowest value of interaction energy (E_{int} = -292.32 kcal·mol^{-1}). The system also exhibits the best inhibition efficiency (82.01%) for carbon steel obtained using a weight loss assay. Moreover, this composition demonstrates the highest synergistic effect (S = 2.59). Individual components demonstrated a negligible protective effect in given corrosion medium. At the same time, most of two-component systems exhibit an antagonistic effect (S < 0). The system consisting of 1,3-phenylenediamine and 1,5-disulfonate demonstrates insignificant additivity (S = 1.05). Thus, both theoretical calculations and experimental methods confirm the high inhibition efficiency and ability to form the binary system between 1.2-PDAH_2^{2+} and 1.5-NDS^{2-} at a molar ratio of 1:1 and total concentration of $1 \cdot 10^{-3}$ mol·dm^{-3}. Therefore, this system was chosen for further, more detailed theoretical and experimental investigation.

At the next step of our research, the proposed binary system was investigated with a different ratio of components at a constant total concentration of the inhibitor ($1 \cdot 10^{-3}$ mol·dm^{-3}). A graphical representation of the obtained results is shown in Figure 1.

As can be seen, the highest inhibition efficiency (82,01%) and synergistic effect (2.59) are demonstrated by a system with a 1:1 component ratio at a total concentration of $1 \cdot 10^{-3}$ mol·dm^{-3} and a concentration of individual components of $5 \cdot 10^{-4}$ mol·dm^{-3}. Furthermore, investigated binary systems demonstrate a synergistic effect at all component ratios, but at a significantly lower level than at a 1:1 molar ratio of the components.

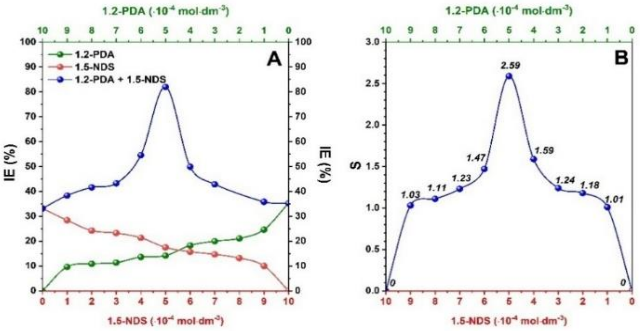

Figure 1 – The inhibitor efficiency of 1,2-phenylenediamine (1.2-PDA) and disodium naphthalene-1,5-sulfonate (1.5-NDS) (A) and synergistic effect (B) at different component ratios on carbon steel in 0.5 mol·dm^{-3} H_2SO_4 solution for 24 hours of immersion

Subsequent determinations of thermodynamic and activation parameters were carried out, maintaining the most effective molar ratio of the binary system components, but at different total concentrations of the inhibitor. Table 2 shows the molar and weight ratios of the components for binary systems at different total concentrations of the inhibitor.

Table 2 – The molar and weight ratios of the 1.2-PDA and 1.5-NDS in binary systems at different total concentrations of the inhibitor.

1,2-PDA		**1,5-NDS**		**Total**	
·10^{-4} mol·dm^{-3}	**g·dm^{-3}**	**·10^{-4} mol·dm^{-3}**	**g·dm^{-3}**	**·10^{-4} mol·dm^{-3}**	**g·dm^{-3}**
2,50	0,0270	2,50	0,0831	5,00	0,1101
3,75	0,0406	3,75	0,1246	7,50	0,1651
5,00	0,0541	5,00	0,1661	10,0	0,2202
12,50	0,1352	12,50	0,4153	25,0	0,5505
25,00	0,2704	25,00	0,8306	50,0	1,1010

For all subsequent results, the total mass of the inhibitor in grams is indicated in accordance with the data in Table 2.

Corrosion parameters of the most effective system.

The weight loss test was performed for different inhibitor concentration at room temperature for a 2-24 hours exposure time. Relationships between corrosion rate and inhibition efficiency with exposure time are shown in Figure 2.

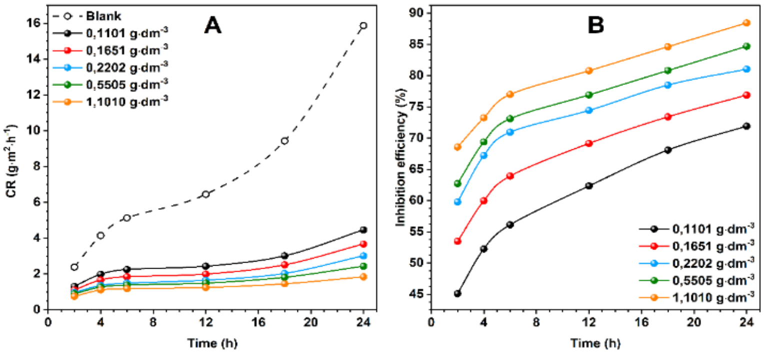

Figure 2 – The relationships between the CR (A), IE (B) and exposure time at different concentration of the binary system of 1,2-PDA and 1.5-NDS on carbon steel in 0.5 mol·dm^{-3} H_2SO_4

Figure 2 shows that in the presence of an inhibitor, the corrosion rate decreases significantly, which leads to a corresponding increase in the inhibition efficiency. With increasing exposure time, the protective effect increases equivalently, reaching a maximum value of 88.43% at the highest inhibitor concentration in 24 hours of immersion. The presence of an insignificant induction period and the subsequent uniform increase in the protective effect until the maximum values are reached indicates that the corrosion inhibitor rapidly adsorbs onto the metal surface and gradually forms a stable, protective layer. This allows to suggest that the inhibitor molecules interact with the metal surface, initiating the adsorption process almost immediately. This behavior is typical of inhibitors that act due to strong physisorption, where the protective effect improves as the surface coverage approaches saturation.

Figure 3 represents corrosion, adsorption, thermodynamics, and activation parameters of 1,2-PDA – 1.5-NDS 1: 1 binary system at 298 and 313K.

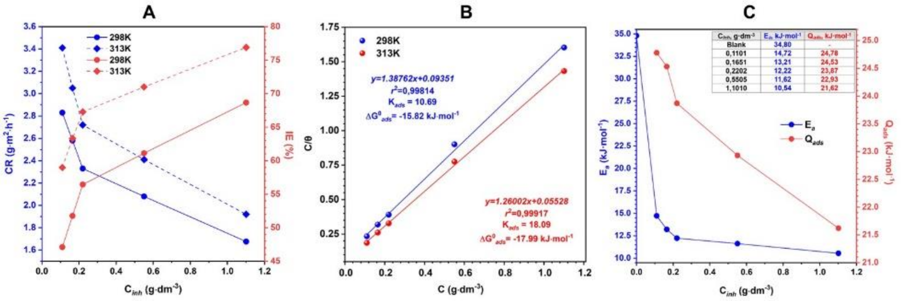

C_{inh}, g·dm^{-3}	E_a, kJ·mol^{-1}	Q_{ads}, kJ·mol^{-1}
Blank	34,80	-
0,1101	14,72	24,78
0,1651	13,21	24,53
0,2202	12,22	23,87
0,5505	11,62	22,93
1,1010	10,54	21,62

Figure 3 – The corrosion rate, and inhibition efficiency (A), the Langmuir adsorption isotherms (B), and variations of the activation energy (E_a) and heat of adsorption (Q_{ads}) (C) at different concentrations of the 1,2-PDA – 1.5-NDS 1: 1 binary system at 298 and 313K for 6 hours immersion period in 0.5 mol·dm^{-3} H_2SO_4 solution (r^2 – linear regression coefficient)

The results demonstrate that increasing temperature enhances the inhibition efficiency (Figure 3A), suggesting sufficient adsorption energy to counteract the elevated kinetic energy of corrosive species, leading to improved surface coverage and a more stable protective layer. Higher inhibitor concentrations further increase protection, indicating that optimal efficiency is achieved at maximum concentration and high temperature. The linear relationship between C and C/θ ($R^2 > 0.995$) confirms that adsorption follows the Langmuir model (Figure 3B), implying monolayer adsorption where inhibitor molecules occupy active metal sites without lateral interactions. Negative Gibbs free energy values indicate spontaneous adsorption, with values near −20 kJ·mol^{-1} suggesting its physical nature (physisorption). The observed decrease in activation energy (E_a) and heat of adsorption (Q_{ads}) with increasing inhibitor concentration (Figure 3C) supports a physisorption mechanism, where the inhibitor forms a protective barrier via weak van der Waals forces, lowering the energy barrier for corrosion. Exceeding Q_{ads} relative to E_a further confirms the formation of a stable protective layer on the metal surface.

Electrochemical experiment

OCP *vs.* time diagram and Tafel polarization curves for carbon steel in 0.5 mol·dm^{-3} H_2SO_4 solution in the presence and absence of various inhibitor concentrations of the inhibitor at room temperature are shown in Figure 4.

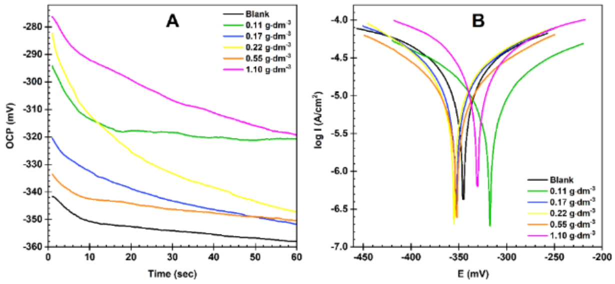

Figure 4 – OCP *vs.* time diagram (A) and Tafel polarization curves (B) for carbon steel in 0.5 mol·dm^{-3} H_2SO_4 solution with and without of the inhibitor at room temperature.

The electrochemical parameters of the corrosion process are presented in Table 3.

As can be seen, the presence of an inhibitor causes a noticeable shift in both the cathodic and anodic sites of the polarization curves, but the shift of the anode sections is more significant, suggesting that the developed composition acts as a mixed-type inhibitor, primarily slowing down the anodic process. As in the gravimetric experiment, the electrochemical experiment shows an increase in the protective effect with an increase in the concentration of the inhibitor. A corresponding increase in the polarization resistance indicates the formation of a protective film on the metal surface and, as a result, a decrease in the rate of corrosion destruction of the metal. The data of the electrochemical measurements are in full agreement with the results of the weight loss experiment.

Table 3 – The electrochemical parameters of carbon steel corrosion in 0.5 mol·dm^{-3} H_2SO_4 in the absence and presence of different concentrations of the inhibitor at room temperature

C_{inh}, g·dm^{-3}	E_{corr}, mV	J_{corr}, A·cm^{-2}	$\|b_a\|$, mV·dec^{-1}	$\|b_c\|$, mV dec^{-1}	R_p, Ω	IE_R, %
0	355,16	$1,16 \cdot 10^{-4}$	94,20	86,76	109,75	-
0,1101	352,69	$1,18 \cdot 10^{-4}$	95,33	87,93	193,97	68,88
0,1651	352,29	$9,28 \cdot 10^{-5}$	83,09	77,66	254,30	76,26
0,2202	345,23	$7,93 \cdot 10^{-5}$	101,50	99,83	305,30	80,23
0,5505	330,57	$6,85 \cdot 10^{-5}$	118,19	97,11	439,46	86,26
1,1010	317,40	$5,35 \cdot 10^{-5}$	85,56	111,51	578,30	89,56

Metal surface analysis

The metal surface was analyzed using optical microscopy and measuring the contact angle. Figure 5 displays microphotographs of the carbon steel surface before and after immersion of carbon steel specimen in 0.5 mol·dm^{-3} H_2SO_4 solution with and without an inhibitor, and corresponding contact angle values.

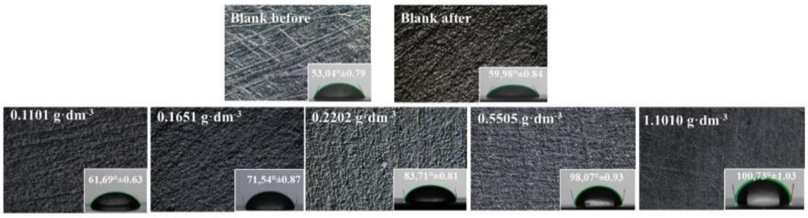

Figure 5 – Micrographs (^{x}50) of the carbon steel surface and contact angle values (inserts) before and after immersing the carbon steel in 0.5 mol·dm^{-3} H_2SO_4 solution for 24 hours in the presence of different inhibitor concentrations

Figure 5 shows that before immersion the surface of a pure metal is uniform and has a metallic luster. After 24 hours of exposure to an uninhibited corrosive environment, the metallic luster disappears completely. The surface of the metal becomes dark and loose with clearly visible damage and pits. In the presence of an inhibitor, the metal surface also loses its metallic luster, but retains its uniformity and clearly identifiable structure. The visible damage of the metal surface decreases with increasing inhibitor concentration, demonstrating the protective effect of the developed inhibitor. A higher contact angle indicates increased hydrophobicity, confirming the adsorption of the inhibitor onto the metal surface. As the experiment showed, the contact angle of a pure metal specimen is 53,04° ± 0.79 which indicates its significant hydrophilicity. After immersion of the metal sample for 24 hours in an uninhibited acid solution, the contact angle was only 59,98° ± 0.84. However, when the metal sample is immersed in an acid solution in the presence of an inhibitor, the contact angle increases significantly, reaching 100,73° ± 1,03 at the maximum concentration of the inhibitor. An increase in the hydrophobicity of the metal surface indicates the formation of a protective film.

Computational results

Optimized structure, mechanism of bonds formation and Mulliken atomic charge distribution (MACD) in ion pair of protonated 1,2-phenylenediamine ($1.2\text{-}PDAH_2^{2+}$), naphthalene-1,5-disulphonate ($1.5\text{-}NDS^{2-}$) at 1:1 ratio calculated with DFT/B3LYP/6-311+G(d,p) method are depicted in Figure 6.

Figure 6 shows that optimized structure of the formed ion pair is characterized by the three-centered (bifurcated) hydrogen bond. The MCDA revealed that formation of hydrogen bonds between $1.2\text{-}PDAH_2^{2+}$ and $1.5\text{-}NDS^{2-}$ at 1: 1 ratio occurs *via* covalently bonded H-atoms of amino group. Hydrogen atoms that have formed a donor-acceptor bond with the nitrogen atoms due to protonation of 1.2-PDA are not involved in the formation of aт intermolecular hydrogen bond with the $1.5\text{-}NDS^{2-}$. The higher tendency of 1,2-phenylenediamine to form ion pairs with sulfonates compared to 1,3- or 1,4- isomers is due to its unique molecular structure when two amino groups are adjacent so that they can simultaneously interact with a single sulfo group through hydrogen bonding. This dual interaction increases the stability of the ion pair by the formation of a three-centered hydrogen bond.

Therefore, the proximity of the amino groups in 1,2-phenylenediamine results in a more favorable charge distribution during protonation, which increases the intermolecular electrostatic interactions. The lowest value of the total negative charge (TNC) calculated for the ion pair clearly indicates its greater tendency to donate electrons to the metal surface and thereby to better exhibit anticorrosive properties. These results are in great agreement with the experimental data.

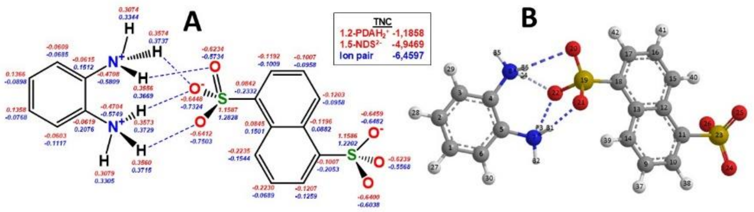

Figure 6 – Structural formula with MACD (A) and optimized structure with atomic enumeration (B) of hydrogen-bonded ion pair of 1.2-PDAH$_2^{2+}$ and 1.5-NDS^{2-} at 1 : 1 ratio (dashed lines represents hydrogen bonds, Mulliken atomic charges of separate individual components are red colored, in ionic pair – blue colored)

Molecular dynamics (MD) simulation

To account for the effect of the metal surface on the mechanism of inhibitor sorption and the formation of a stable ion pair, molecular dynamic modeling was performed. For this purpose, the adsorption energies were calculated for a system containing individual components and for a system containing an ion pair. The lowest energy configurations of both systems are presented in Figure 7.

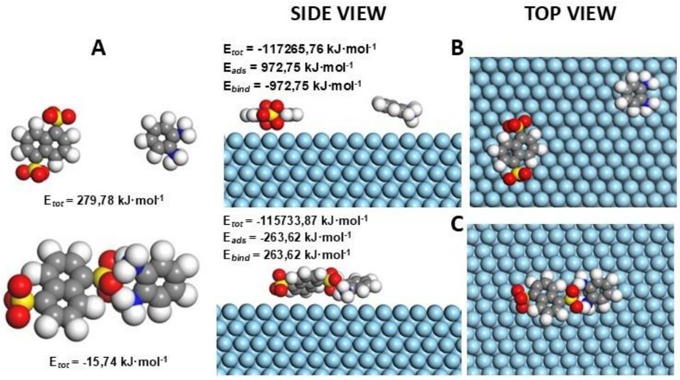

Figure 7 – View of binary system of pair of 1.2-PDAH$_2^{2+}$ and 1.5-NDS^{2-} at 1: 1 ratio as individual components and hydrogen-bonded ion pair (A), and side and top views of the most appropriate configuration for adsorption of system of individual inhibitor components (B) and hydrogen-bonded ion pair (C) on Fe(110) surface.

Molecular dynamics simulations reveal that individual inhibitor components adsorb onto the Fe(110) surface, and this system exhibits a positive adsorption energy (972.75 kJ·mol^{-1}), indicating a tendency toward desorption. In contrast, when the system presents as an ion pair, the adsorption energy becomes negative (-263.62 kJ·mol^{-1}), favoring adsorption. Using Hess's law, the energy required to form the ion pair in solution is calculated as -295.62 kJ·mol^{-1}, and -1531.89 kJ·mol^{-1} on Fe(110) surface, unequivocally emphasizes that the joint sorption of inhibitor components on the metal surface contributes to the formation of an ion pair and increases the inhibition efficiency. The formation of an intermolecular hydrogen bond upon adsorption strengthens the protective layer, emphasizing the synergistic effect of the inhibitor components in improving overall inhibition efficiency.

Conclusion

This study introduces a novel binary system comprising 1,2-phenylenediamine and disodium naphthalene-1,5-sulfonate, which demonstrates great corrosion inhibition efficiency for carbon steel in 0.5 mol·dm^{-3} H_2SO_4. Experimental results revealed that the system achieves a maximum inhibition efficiency of 88.43% under optimal conditions, with a synergistic effect parameter of 2.59.

The protective mechanism is attributed to the formation of a stable ion pair through intermolecular hydrogen bonding directly on the metal surface, as confirmed by molecular dynamics simulations and DFT calculations. Adsorption studies indicated monolayer adsorption, in accordance with the Langmuir isotherm, and thermodynamic parameters confirmed spontaneous physisorption. Electrochemical analysis identified the binary system as a mixed-type inhibitor, primarily reducing the anodic reaction. Surface characterization further validated the formation of a dense protective film, enhancing hydrophobicity and reducing corrosion damage. The results obtained indicate that the formation of an effective inhibitor is possible not only directly in solution but also on the metal surface. Such additional stabilization of the structure makes the resulting ion pair more stable, thereby increasing the overall effectiveness of the inhibitor.

References

1. Kazieva R.Yu. Heteroorganic compounds are effective corrosion inhibitors of metal equipment / R.Yu. Kazieva, N.R. Abdullayeva, L.I. Aliyeva // Oil and Gas Business. – 2024. – № 2. – P. 141-166. https://doi.org/10.17122/ogbus-2024-2-141-166.
2. Ahmed M.A. Current and emerging trends of inorganic, organic and eco-friendly corrosion inhibitors / M.A. Ahmed, S. Amin, A.A. Mohamed // RSC advances. – 2024. – T. 14, № 43. – P. 31877-31920. https://doi.org/10.1039/D4RA05662K.
3. Kosmina M.M. Evaluation of the Effectiveness of Inhibitor Protection of Metal Surfaces in Aggressive Water-Oil Environments / M.M. Kosmina, Yu.V. Nosachova, T.O. Shablii // Bulletin of NTUU «Igor Sikorsky KPI». Series: Chemical Engineering, Ecology, and Resource Conservation. – 2024. – № 4. – P. 62-68. https://doi.org/10.20535/2617-9741.4.2024.319148.
4. Development of green vapour corrosion inhibitor / Y.P. Asmara et al // IOP Conference Series: Materials Science and Engineering. – IOP Publishing. – 2017. – T. 257, № 1. – P. 012089. https://doi.org/10.1088/1757-899X/257/1/012089.
5. Molecular modelling of compounds used for corrosion inhibition studies: a review / E.E. Ebenso et al // Physical Chemistry Chemical Physics. – 2021. – T. 23, № 36. – P. 19987-20027. https://doi.org/10.1039/d1cp00244a.
6. Javadian S. Synergistic effect of mixed cationic and anionic surfactants on the corrosion inhibitor behavior of mild steel in 3.5% NaCl / S. Javadian, A. Yousefi, J. Neshati // Applied Surface Science. – 2013. – T. 285. – P. 674-681. http://dx.doi.org/10.1016/j.apsusc.2013.08.109.
7. The synergistic effect of sodium phytate and benzotriazole as corrosion inhibitors of 20SiMn steel in 3.5 wt-% NaCl solution / F. Cao et al // Corrosion Engineering, Science and Technology. – 2023. – T. 58, № 1. – P. 36-48. https://doi.org/10.1080/1478422X.2022.2132616.
8. Aminocarboxylate corrosion inhibitors of carbon steel in tap water / E. Amangeldieva et al // Engineering Journal of Satbayev University. – 2022. – T. 144, № 5. – P. 11-18. https://doi.org/10.51301/ejsu.2022.i5.02.
9. Черная смородина (*Ribes Nigrum*) из Западного Казахстана – новый природный экологически чистый ингибитор коррозии углеродистой стали / Н.В. Акатьев и др. // Вестник Университета Шакарима. Серия технические науки. – 2024. – Т. 1, № 2(14). – С. 390-401. https://doi.org/10.53360/2788-7995-2024-2(14)-49.
10. Development of new three-component BNP-inhibitor for carbon steel in 0.5 mol dm-3 HCl solution, Thermodynamic, adsorption and electrochemical studies / T. Seilova et al // The International Journal of Corrosion and Scale Inhibition. – 2024. – № 13. – P. 1268-1291.
11. General atomic and molecular electronic structure system / M.W. Schmidt et al // Journal of computational chemistry. – 1993. – T. 14, № 11. – P. 1347-1363. https://doi.org/10.1002/jcc.540141112.
12. Klamt A. The COSMO and COSMO-RS solvation models / A. Klamt // WIREs Computational Molecular Science. – 2017. – № 8(1). – P. e1338. https://doi.org/10.1002/wcms.1338.
13. GROMACS: High performance molecular simulations through multi-level parallelism from laptops to supercomputers / M.J. Abraham et al // SoftwareX. – 2015. – № 1. – P. 19-25. https://doi.org/10.1016/j.softx.2015.06.001.
14. Density functional theory and molecular dynamics simulation studies of bio-based fatty hydrazide-corrosion inhibitors on Fe (110) in acidic media / N. Mazlan et al; // Journal of Molecular Liquids. – 2022. – № 347(1). – P. 118321. https://doi.org/10.1016/j.molliq.2021.118321.

Р. Кенжегалиева, М. Жолдыбаев, Н. Акатьев*
Западно-Казахстанский университет им. М. Утемисова,
090000, Республика Казахстан, Уральск, пр. Н. Назарбаева, 162
*e-mail: nikolay.akatyev@wku.edu.kz

СИНЕРГЕТИЧЕСКИЙ ЭФФЕКТ 1,2-ФЕНИЛЕНДИАМИНА И НАФТАЛИН-1,5-ДИСУЛЬФОНАТА НАТРИЯ ДЛЯ УСИЛЕННОЙ ЗАЩИТЫ УГЛЕРОДИСТОЙ СТАЛИ ОТ КОРРОЗИИ В 0,5 М РАСТВОРЕ H_2SO_4: ЭКСПЕРИМЕНТАЛЬНЫЕ И ТЕОРЕТИЧЕСКИЕ ВЫВОДЫ

В данной работе исследуется ингибирование коррозии углеродистой стали в среде в 0,5 М растворе H_2SO_4 с использованием бинарной системы 1,2-фенилендиамина и нафталин-1,5-дисульфоната натрия. Экспериментальные методы, включая метод потери массы, электрохимические методы и анализ поверхности, продемонстрировали значительную эффективность ингибирования, достигающую 88,43% при оптимальных условиях. Синергетический эффект между двумя компонентами составил 2,59, что указывает на значительное повышение эффективности по сравнению с отдельными компонентами. Расчётные исследования с использованием методов молекулярной динамики и DFT выявили сильные взаимодействия, обусловленные образованием водородных связей под действием электростатических сил во время адсорбции, которые стабилизируют защитный слой на поверхности металла. Механизм адсорбции соответствовал модели адсорбции Ленгмюра, а полученные термодинамические параметры подтвердили самопроизвольную физическую адсорбцию ингибитора. Результаты электрохимического анализа показали, что бинарная система является ингибитором смешанного типа, эффективно снижающим процессы как анодной, так и катодной коррозии. Эти результаты дают ценную информацию о разработке синергетических систем ингибиторов для промышленного применения.

Ключевые слова: *защита металлов, синергетический эффект, ингибиторы коррозии, эффективность ингибирования, молекулярная динамика, дескрипторы реакционной способности.*

Р. Кенжегалиева, М. Жолдыбаев, Н. Акатьев*
Батыс Қазақстан университеті. М. Өтемісова,
090000, Қазақстан Республикасы, Орал, Н. Назарбаев даңғылы, 162
*e-mail: nikolay.akatyev@wku.edu.kz

0,5 М H2SO4 ЕРІТІНДІСІНДЕГІ КӨМІРТЕКТІ БОЛАТТЫ КОРРОЗИЯДАН ҚОРҒАУДЫ КҮШЕЙТУ ҮШІН 1,2-ФЕНИЛЕНДИАМИН МЕН НАФТАЛИН-1,5-НАТРИЙ ДИСУЛЬФОНАТЫНЫҢ СИНЕРГЕТИКАЛЫҚ ӘСЕРІ: ЭКСПЕРИМЕНТТІК ЖӘНЕ ТЕОРИЯЛЫҚ ТҰЖЫРЫМДАР

Бұл жұмыс 1,2-фенилендиамин мен нафталин-1,5-натрий дисульфонатының бинарлы жүйесін қолдана отырып, 0,5 М H_2SO_4 ерітіндісіндегі көміртекті болаттың коррозиясын тежеуді зерттейді. Эксперименттік әдістер, соның ішінде массаны жоғалту әдісі, электрохимиялық әдістер және беттік талдау оңтайлы жағдайларда 88,43% - ға жететін тежелудің айтарлықтай тиімділігін көрсетті. Екі компонент арасындағы синергетикалық әсер 2,59 құрады, бұл жеке компоненттермен салыстырғанда тиімділіктің айтарлықтай жақсарғанын көрсетеді. Молекулалық динамика және DFT әдістерін қолданатын есептелген зерттеулер адсорбция кезінде электростатикалық күштердің әсерінен сутегі байланыстарының түзілуіне байланысты күшті өзара әрекеттесулерді анықтады, бұл металл бетіндегі қорғаныс қабатын тұрақтандырады. Адсорбция механизмі Ленгмюр адсорбция үлгісіне сәйкес келді және алынған термодинамикалық параметрлер ингибитордың өздігінен физикалық адсорбциясын растады. Электрохимиялық талдау нәтижелері екілік жүйенің анодты және катодты коррозия процестерін тиімді төмендететін аралас типті ингибитор екенін көрсетті. Бұл нәтижелер өнеркәсіптік қолдануға арналған синергетикалық ингибиторлық жүйелердің дамуы туралы құнды ақпарат береді.

Түйін сөздер: *металды қорғау, синергетикалық әсер, коррозия ингибиторлары, ингибирлеу тиімділігі, молекулалық динамика, реактивтілік дескрипторлары*

Information about the authors

Nikolay Vladimirovich Akatyev* – candidate of chemical sciences, senior lecturer, M.Utemisov West Kazakhstan university, Uralsk, Republic of Kazakhstan; e-mail: nikolay.akatyev@wku.edu.kz. ORCID: https://orcid.org/0000-0001-9248-2753.

Roza Zhalgasovna Kenzhegalieva – master student, M. Utemisov West Kazakhstan university, Uralsk, Republic of Kazakhstan; e-mail: rozka_k90@mail.ru. ORCID: https://orcid.org/0009-0007-9236-6155.

Majan Kobylandyuly Zholdybayev – 4th year students, M. Utemisov West Kazakhstan university, Uralsk, Republic of Kazakhstan; e-mail: gumarovkobylandy@gmail.com. ORCID: https://orcid.org/0009-0004-5948-3868.

Авторлар туралы мәліметтер

Николай Владимирович Акатьев* – химических ғылымдарының кандидаты, аға оқытушы, М. Өтемісов атындағы Батыс Қазақстан университеті, Орал қ., Қазақстан; e-mail: nikolay.akatyev@wku.edu.kz. ORCID: https://orcid.org/0000-0001-9248-2753.

Роза Жалгасовна Кенжегалиева – магистрант, М. Өтемісов атындағы Батыс Қазақстан университеті, Орал қ., Қазақстан; e-mail: rozka_k90@mail.ru. ORCID: https://orcid.org/0009-0007-9236-6155.

Маджан Қобыландыұлы Жолдыбаев – 4 курс студенті, М. Өтемісов атындағы Батыс Қазақстан университеті, Орал қ., Қазақстан; e-mail: gumarovkobylandy@gmail.com. ORCID: https://orcid.org/0009-0004-5948-3868

Сведения об авторах

Николай Владимирович Акатьев* – кандидат химических наук, старший преподаватель, Западно-Казахстанский университет им. М. Утемисова, г. Уральск, Республика Казахстан; e-mail: nikolay.akatyev@wku.edu.kz. ORCID: https://orcid.org/0000-0001-9248-2753.

Роза Жалгасовна Кенжегалиева – магистрант, Западно-Казахстанский университет им. М. Утемисова, г. Уральск, Республика Казахстан; e-mail: rozka_k90@mail.ru. ORCID: https://orcid.org/0009-0007-9236-6155.

Маджан Кобландыулы Жолдыбаев – студент 4 курса, Западно-Казахстанский университет им. М. Утемисова, г. Уральск, Республика Казахстан; e-mail: gumarovkobylandy@gmail.com. ORCID: https://orcid.org/0009-0004-5948-3868.

Received 01.04.2025
Accepted 12.05.2025

---

https://doi.org/10.53360/2788-7995-2025-2(18)-63

МРНТИ: 61.51.17

Е.И. Иманбаев[1]*, А.К. Серикказинова[1], Д. Мукталы[1], А.Ш. Аккенжеева[2], А.Ч. Бусурманова[2]
[1]Институт проблем горения,
Республика Казахстан, г. Алматы, ул. Богенбай батыра, 172
[2]Каспийский университет технологий и инжиниринга имени Ш. Есенова,
Республика Казахстан, г. Актау, 32-й микрорайон, 1
*e-mail: erzhan.imanbayev@mail.ru

ИСПОЛЬЗОВАНИЕ СВЕРХКРИТИЧЕСКИХ ФЛЮИДОВ В НЕФТЕПЕРЕРАБОТКЕ

Аннотация: *На сегодняшний день в мире нефтяная промышленность по своей деятельности особое внимание уделяет развитию новых подходов переработки, повышению энергоэффективности и снижению эксплуатационных затрат. Обзор рассматривает современные методы переработки тяжелых нефтей с использованием сверхкритических флюидов. Основное внимание уделяется сверхкритической флюидной экстракции, которые позволяют эффективно извлекать углеводороды и удалять нежелательные примеси. В обзоре рассмотрены кинетика взаимодействия сверхкритических флюидов, а также влияние температуры, давления и растворителей на эффективность сверхкритической флюидной экстракции. Ключевые особенности данного метода являются глубина очистки, селективность процессов, высокая избирательность, снижение отходов, возможность регенерации растворителей, сокращение выбросов и уменьшение негативного воздействия на окружающую среду. Однако в использовании сверхкритических флюидов в нефтяной промышленности имеются определенные ограничения, включая высокие энергозатраты, необходимость сложного оборудования и технологические сложности при масштабировании процессов, что требует дальнейших исследований и оптимизации параметров. Рассмотрены перспективы интеграции сверхкритической флюидной технологий в нефтеперерабатывающую промышленность, включая комбинированные методы с катализаторами и модификаторами растворителей. Установлено, что внедрение сверхкритической флюидной технологий в нефтяную отрасль может значительно повысить эффективность переработки тяжелых углеводородных систем, способствуя созданию более экологичных и экономически устойчивых технологий.*

Ключевые слова: *сверхкритические флюиды, переработка, сверхкритическая флюидная экстракция, растворитель, нефтебитуминозные породы.*